Modeling and Sensitivity Study of Consensus Algorithm-Based Distributed Hierarchical Control for DC Microgrids

Meng, Lexuan; Dragicevic, Tomislav; Roldan Perez, Javier; Vasquez, Juan Carlos; Guerrero, Josep M.

Published in:
I E E E Transactions on Smart Grid

DOI (link to publication from Publisher):
10.1109/TSG.2015.2422714

Publication date:
2016

Document Version
Early version, also known as pre-print

Modeling and Sensitivity Study of Consensus Algorithm Based Distributed Hierarchical Control for DC Microgrids

Lexuan Meng, *Student Member, IEEE*, Tomislav Dragicevic, *Member, IEEE*, Javier Roldán-Pérez, *Member, IEEE*, Juan C. Vasquez, *Senior Member, IEEE* and Josep M. Guerrero, *Fellow, IEEE*

***Abstract*--Distributed control methods based on consensus algorithms have become popular in recent years for microgrid (MG) systems. These kinds of algorithms can be applied to share information in order to coordinate multiple distributed generators within a MG. However, stability analysis becomes a challenging issue when these kinds of algorithms are used, since the dynamics of the electrical and the communication systems interact with each other. Moreover, the transmission rate and topology of the communication network also affect the system dynamics. Due to discrete nature of the information exchange in the communication network, continuous-time methods can be inaccurate for this kind of dynamic study. Therefore, this paper aims at modeling a complete DC MG using a discrete-time approach in order to perform a sensitivity analysis taking into account the effects of the consensus algorithm. To this end, a generalized modeling method is proposed and the influence of key control parameters, the communication topology and the communication speed are studied in detail. The theoretical results obtained with the proposed model are verified by comparing them with the results obtained with a detailed switching simulator developed in Simulink/Plecs.**

***Index Terms*--DC microgrids, DC/DC converters, consensus algorithm, distributed hierarchical control, discrete-time modeling.**

I. Introduction

Microgrid (MG) concept is commonly proposed for an efficient aggregation and exploitation of distributed resources (DR), storage systems and consumers [1]. MGs can operate either islanded or connected to the grid, thus increasing the flexibility and security of the electrical system. A great number of methods have been proposed to achieve typical MG control objectives, such as equal power sharing, enhanced power quality, optimized energy efficiency and DR coordination [2]–[4].

Hierarchical controllers [2], [3] are commonly applied to MGs to achieve multiple control objectives at the same time, but in different time scales. The primary controller provides an adequate power sharing among DRs. The local droop is usually in this control level and it is a fashionable way to achieve distributed power sharing in the short-term without communications. The secondary controller can help improving the power quality of a MG and it can also provide ancillary services. This kind of control hierarchy can be implemented in centralized [2], [5], [6] or distributed fashion [7]–[9]. In the top level, a tertiary controller manages the power flow of the MG and optimizes economic issues. A method to optimize the efficiency is proposed in [10]. Here, a genetic algorithm is implemented in the tertiary controller to minimize the losses of the whole system. Other types of centralized energy management controllers are studied in the literature [11]–[14]. On the other hand, several attempts have been made to achieve distributed management [15]–[17]. For that matter, consensus algorithm [18] is often used since it facilitates the information synthesis and aggregation among a set of distributed agents.

For both the secondary and the tertiary controllers, low bandwidth communication links (LBCL) are commonly used for data transmission [19]. In general, when considering the initial investment in the communication network, as well as flexibility and reliability of the system, distributed control methods are usually preferred. They offer the advantages like: 1) communication is only needed between neighboring units; 2) the risk of overall system failure can be reduced since there is no central control unit and the length of communication links can be shortened.

In order to achieve fully distributed control, this paper applies a dynamic consensus algorithm (DCA) [20] based distributed hierarchical control method to realize accurate current sharing and voltage restoration. Up to date, several kinds of current sharing approaches were proposed, such as droop control and master-slave control [3], [21], [22]. Master-slave control facilitates the well sharing of load current, however, a single point of failure (SPOF) of the master unit compromises the safety of the entire system [22]. Droop control can achieve communication-less current sharing among converters, but voltage deviation and current sharing error usually exist. On top of droop control, conventional centralized secondary control can be implemented to eliminate those errors, but the issue of SPOF still exists in the central controller [3]. Also communication links are required from the central control to every local unit which causes high communication cost, and lower reliability and flexibility.

Lexuan Meng, Tomislav Dragicevic, Josep M. Guerrero, Juan C. Vásquez are with Department of Energy Technology, Aalborg University, 9220 Aalborg, Denmark (e-mail: {lme,tdr,joz,juq}@et.aau.dk).

Javier Roldán Pérez is with School of Engineering, Comillas Pontifical University, Alberto Aguilera 23, 28015 Madrid, Spain (email: Javier.Roldan@iit.upcomillas.es)

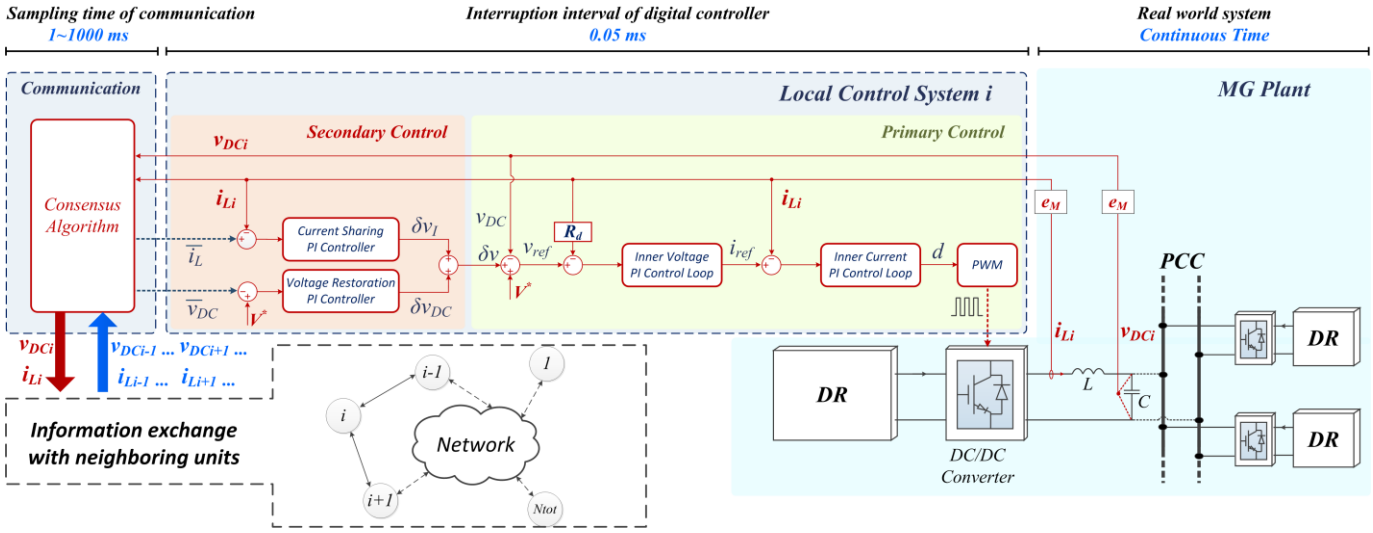

Fig. 1. Distributed hierarchical control for DC microgrids.

Compared with above mentioned methods, the approach applied in this paper is a fully distributed control method avoiding the problem of SPOF, and communication links are only required between nearby units. System flexibility is enhanced with plug-and-play function.

Moreover, the inclusion of consensus algorithm in the finite-speed-communication links becomes a challenge when paired with dynamics of electrical network. In the existing studies [7], [9], consensus algorithm is modeled with MG system in continuous domain, the correctness and accuracy of which has never been evaluated. Considering the discrete nature of communication system and different feature of electrical, digital control and communication network, *s*-domain continuous-time (CT) model is then not accurate enough to represent the overall system behavior. The electrical part, which includes the filter, transmission lines and loads, is actually a CT system, while the digital controller and communication network are discrete-time (DT) systems. Moreover, sampling times of control and communication (for communication part sampling time corresponds to transmission rate) significantly differ with typical times for the matter being in μs range and ms range respectively. In order to analyze this kind of system, *z*-domain DT modeling is applied in this paper taking into account the discrete nature of measurement, controller implementation and communication.

A DC MG with primary and secondary control is taken as the study case. Consensus algorithm is used for information sharing among DRs. The paper is organized as follows. Section II introduces the principles of distributed hierarchical control for DC MGs including primary and secondary control levels. The basics of consensus algorithm are presented in Section III. Section IV proposes the modeling method, based on which the system state space (SS) model is established. Section V shows the comparison of the SS model with Simulink/Plecs (SP) simulation results, and the sensitivity of overall system is studied considering the secondary control parameters, communication speed and topological variations. Section VI gives the conclusion.

II. Consensus Algorithm based Distribute Hierarchical Control Scheme

The consensus algorithm based distributed hierarchical control scheme for a DC MG is shown in Fig. 1. A DR is connected through an interfacing DC/DC converter with an *LC* filter to the point of common coupling (PCC), which also serves as an interface to the loads.

The local control system includes primary control loops and secondary control loops. Primary control is in charge of voltage and current regulation. Proportional integral (PI) controllers are used in inner voltage and current control loops:

$$d = (\frac{K_{ic}}{s} + K_{pc}) \cdot (i_{ref} - i_{Li}) \tag{1}$$

$$i_{ref} = (\frac{K_{iv}}{s} + K_{pv}) \cdot (V^* + \delta v - v_{DC} - i_{Li} R_d) \tag{2}$$

where s is the *Laplace* operator, d is the duty ratio for pulse width modulation (PWM), i_{ref} is the current reference, V^* is the voltage reference, δv is the compensating voltage term generated by secondary control, v_{DC} and i_{Li} are the measured PCC voltage and output current, K_{ic} and K_{pc} are the integral and proportional term of current PI controller, K_{iv} and K_{pv} are the integral and proportional term of voltage PI controller. A virtual resistance R_d feedback (often referred to as the droop control [2], [3]) is also implemented to achieve decentralized current sharing and enhance system damping.

However, voltage deviation inevitably appears when droop control is applied. Also, the load current cannot be accurately shared when transmission lines have differences in parameters or the measurements of different DR units have errors. Secondary control can be installed to avoid these problems:

$$\delta v_I = (\frac{K_{isc}}{s} + K_{psc}) \cdot (\bar{i}_L - i_{Li}) \tag{3}$$

$$\delta v_{DC} = (\frac{K_{isv}}{s} + K_{psv}) \cdot (V^* - \bar{v}_{DC}) \tag{4}$$

where δv_I and δv_{DC} are the compensating terms for current sharing and voltage restoration, respectively. $\bar{i}_L$ and $\bar{v}_{DC}$ are

the averaged output current and PCC voltage of all the DR units, and they are obtained by using consensus algorithm which is introduced in the next Section. K_{isc} and K_{psc} are the integral and proportional term of current sharing controller, K_{isv} and K_{psv} are the integral and proportional term of voltage restoration controller. The summation of δv_I and δv_{DC} is sent to primary controller.

On the top of the controller, consensus algorithm is implemented for information sharing and averaging among a set of distributed agents. It helps to discover the averaged value of total generation current $\bar{i}_L$ and measured PCC voltage $\bar{v}_{DC}$. This part is explained in detail in the following section.

III. Dynamic Consensus Algorithm

Consensus problems and algorithms find their roots in the computer science area [23]. In recent years, they have been more and more applied in multi-agent and multi-vehicle systems [9], [15]–[18]. The general purpose of consensus algorithm is to allow a set of distributed agents to reach an agreement on a quantity of interest by exchanging information through communication network. In case of MG systems, these algorithms can be used to achieve the information sharing and coordination among distributed units. *Graph Laplacians* [24] describe the underlying communication structure in these kinds of systems and play a pivotal role in their convergence and dynamic analysis.

A. Dynamic Consensus Algorithm

The basic consensus algorithm with continuous-time and discrete-time integrator agents can be described as [18], [23]:

$$\dot{x}_i(t) = \sum_{j\in N_i} a_{ij}\cdot(x_j(t)-x_i(t)) \tag{5}$$

$$x_i(k+1) = x_i(k) + \varepsilon\cdot\sum_{j\in N_i} a_{ij}\cdot(x_j(k)-x_i(k)) \tag{6}$$

where i=1,2,…,N_T, N_T is the total number of agent nodes. x_i is the state of agent i. a_{ij} indicates the connection status between node i and node j, a_{ij}=0 if the nodes i and j are not linked. N_i is the set of indexes of the agents that can be connected with agent i, and ε is the constant edge weight used for tuning the dynamic of DCA.

Considering the discrete nature of communication data transmission, DT form of the consensus algorithm (eq. (6)) is used in this paper. In addition, in order to ensure the accurate consensus in dynamically changing environment, a modified version of the algorithm, referred to as dynamic consensus algorithm (DCA) [20], is applied in this paper (see Fig. 2):

$$x_i(k+1) = x_i(0) + \varepsilon\cdot\sum_{j\in N_i}\delta_{ij}(k+1) \tag{7}$$

$$\delta_{ij}(k+1) = \delta_{ij}(k) + a_{ij}\cdot\left(x_j(k)-x_i(k)\right) \tag{8}$$

where $\delta_{ij}(k)$ stores the cumulative difference between two agents, and $\delta_{ij}(0)=0$. Based on (7) and (8), it is explicit that the final consensus value depends on initial value $x_i(0)$, and regardless of any changes to $x_i(0)$, the algorithm will converge to an appropriate average value.

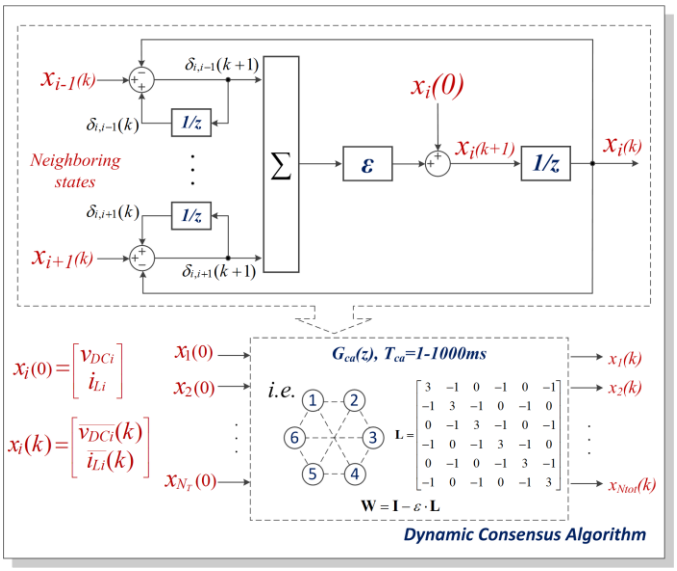

Fig. 2. Dynamic consensus algorithm model

From the system point of view, vector form of the iteration algorithm can be expressed as [18], [23]:

$$\mathbf{x}(k+1) = \mathbf{W}\cdot\mathbf{x}(k) \tag{9}$$

where $\mathbf{x}$ is the state vector $\mathbf{x}(k)=[x_1(k),x_2(k),...,x_{N_T}(k)]^T$ and $\mathbf{W}$ is the weight matrix of the communication network. If a constant edge weight ε is considered, $\mathbf{W}$ can be described as:

$$\mathbf{W} = \mathbf{I} - \varepsilon\cdot\mathbf{L} \tag{10}$$

$$\mathbf{L} = \begin{bmatrix} \sum_{j\in N_1} a_{1j} & \cdots & -a_{1N_T} \\ \vdots & \ddots & \vdots \\ -a_{1N_T} & \cdots & \sum_{j\in N_T} a_{N_T j} \end{bmatrix} \tag{11}$$

where $\mathbf{L}$ is the laplacian matrix of the communication network [25], [26], N_i is the set of indexes of the agents that are connected with agent i and N_T is the total number of agents. The final consensus equilibrium $\mathbf{x}_{eq}$ is:

$$\mathbf{x}_{eq} = \lim_{k\to\infty}\mathbf{x}(k) = \lim_{k\to\infty}\mathbf{W}^k\mathbf{x}(0) = \left(\frac{1}{N_T}\mathbf{1}\cdot\mathbf{1}^T\right)\mathbf{x}(0) \tag{12}$$

where $\mathbf{x}(0)=[\mathbf{x}_1(0),\mathbf{x}_2(0),...,\mathbf{x}_{N_T}(0)]$ is the vector of the initial values held by each agent, $\mathbf{1}$ denotes a vector where all the components equals one. The detailed proof of the algorithm convergence can be found in [18]. In this paper, the initial values are the locally measured PCC voltage (v_{DCi}) and the inductor current (i_{Li}).

B. Algorithm convergence and dynamic

In order to ensure the stability and fast convergence of the communication algorithm ε has to be properly chosen. Assuming that the communication links are bidirectional, the problem of finding the fastest rate is referred as “the symmetric fastest distributed linear averaging” (*symmetric FDLA*) problem. This problem it is actually the minimization of spectral radius of the matrix $\mathbf{W}-(1/N_T)\cdot\mathbf{1}\cdot\mathbf{1}^T$ with certain constraints on the weight matrix $\mathbf{W}$. The fastest convergence is obtained when the following condition is fulfilled [27]:

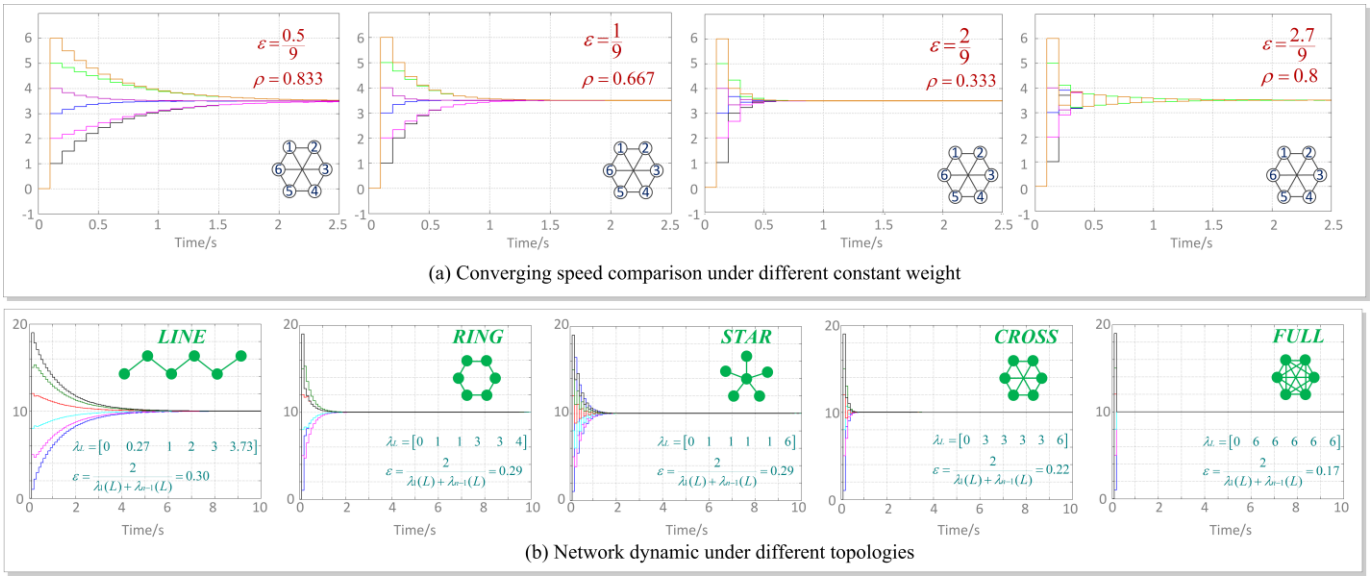

Fig. 3. Dynamic consensus algorithm based network dynamic.

$$\varepsilon = \frac{2}{\lambda_1(L)+\lambda_{n-1}(L)} \tag{13}$$

where $\lambda_j(\cdot)$ denotes the j^{th} largest eigenvalue of a symmetric matrix. Based on the topology of Fig. 2, the eigenvalues of L are $[0\ 3\ 3\ 3\ 3\ 6]^T$, which gives the optimal ε =2/9. The convergence speed is compared in Fig. 3 (a) as an example. In this case, the sampling time of the consensus algorithm is set to T_{ca}=100ms. The system starts with $\mathbf{x}(0)=[1,2,3,4,5,6]$ and converges to average value 3.5. According to the results in Fig. 3 (a), the constant edge weight ε has a pivotal influence over the dynamics of the DCA and, when ε =2/9, the spectral radius $\rho(\mathbf{W}-(1/N_T)\cdot\mathbf{1}\cdot\mathbf{1}^T)$ is minimum and the fastest transient response is achieved.

The topology of the communication network also has influence on the system dynamics, as shown in Fig. 3 (b). In this analysis, five topologies are considered: LINE shaped, RING shaped, STAR shaped, CROSS shaped and fully connected networks. For all cases, the fastest convergence is obtained when the value of ε is selected according to (13) (the optimal value of for each case is given the figure). Results indicate that the communication topology has a big impact on the network dynamics. Obviously, fully-connected network offers the fastest convergence speed, but the cost of the communication network is very high and thus impractical in most of the situations.

IV. System Modeling

A block diagram of the complete system is depicted in Fig. 4. In that figure, each color stands for a part of the system: 1) model of the MG $\boldsymbol{G_{plt}}$(s) (DR, converters, filter and loads), 2) controllers of the converters $\boldsymbol{G_{ctrl}}$(s) (primary control and secondary control) and 3) communication network $\boldsymbol{G_{ca}}$(s) (consensus algorithm and communication topology).

A. Microgrid plant

The generalized DC MG plant is shown in Fig. 5. DR is simplified as a DC source, which is connected to PCC through

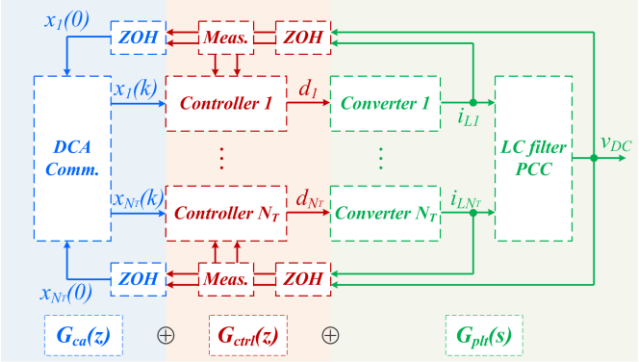

Fig. 4. Structure of complete system model.

a DC/DC converter and LC filter. Synchronous buck converters are used in this particular study case. They convert input voltage v_{in} to output voltage v_o that appears at the common DC bus. Resistive loads (R_{load}) that are also connected to PCC are considered in this paper. Averaged model of the DC/DC converter is used. If a total number of N_T DRs and converters are connected in parallel, the plant model can be described as:

$$i_{Li}(t) = \frac{1}{sL}\cdot\left(v_{in}\cdot d(t) - v_{DC}(t)\right) \tag{14}$$

$$v_{DC}(t) = \frac{1}{N_T\cdot sC}\cdot\left(\sum i_{Li}(t) - \frac{v_{DC}(t)}{R_{load}}\right) \tag{15}$$

The transfer funtion $G_{plt}(s)$ contains the relationship between duty ratios [d_1, d_2, …, d_{NT}] (inputs), inductor currents [i_{L1}, i_{L2}, …, i_{LNT}] and PCC voltages v_{DC} (outputs). The SS model of the MG plant part is:

$$\begin{cases}\dot{\mathbf{x}}_{\mathbf{plt}}(t) = \mathbf{A.plt}\cdot\mathbf{x}_{\mathbf{plt}}(t) + \mathbf{B.plt}\cdot\mathbf{u}_{\mathbf{plt}}(t)\\ \mathbf{y}_{\mathbf{plt}}(t) = \mathbf{C.plt}\cdot\mathbf{x}_{\mathbf{plt}}(t) + \mathbf{D.plt}\cdot\mathbf{u}_{\mathbf{plt}}(t)\end{cases} \tag{16}$$

$$\mathbf{x}_{plt}(t) = \begin{bmatrix} i_{L1}(t) & \cdots & i_{LNT}(t) & v_{DC}(t)\end{bmatrix}^T$$

$$\mathbf{u}_{plt}(t) = \begin{bmatrix} d_1(t) & \cdots & d_{NT}(t)\end{bmatrix}^T \tag{17}$$

$$\mathbf{y}_{plt}(t) = \begin{bmatrix} i_{L1}(t) & \cdots & i_{LNT}(t) & v_{DC}(t)\end{bmatrix}^T$$

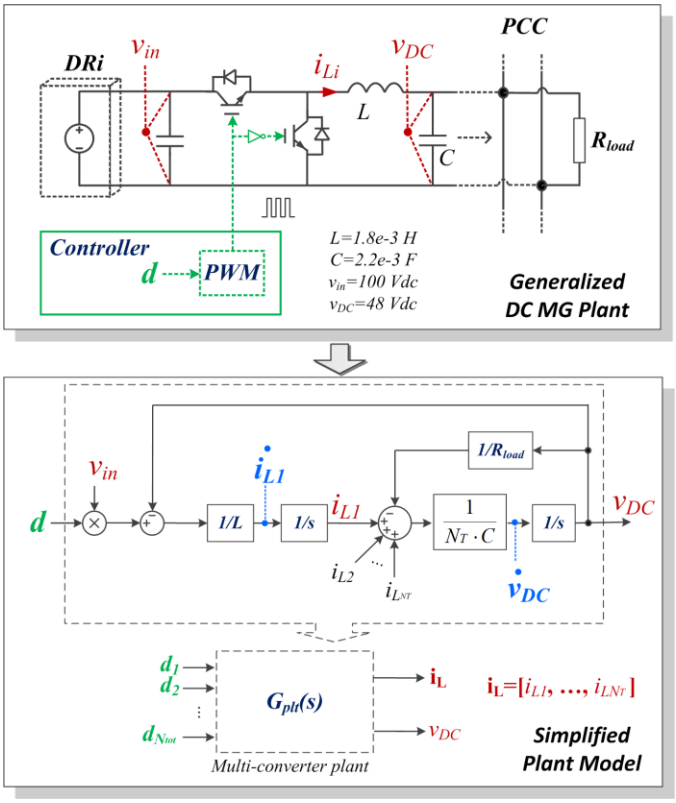

Fig. 5. DC MG plant model.

where **A.plt**, **B.plt**, **C.plt** and **D.plt** are the *state matrix*, the *input matrix*, the *output matrix* and the *feedthrough matrix*, respectively.

B. Controller

The controller diagram is shown in Fig. 1. Four PI control loops and a droop control loop are included as described in (1)-(4). A local error e_M (%) is also considered which can be caused by transmission line parameter differences or measurement error.

A transfer function $G_{ctrl}(s)$ is obtained. The input variables are voltage reference (V^*), averaged measured PCC voltage obtained by each local controller by using DCA ($\bar{v}_{DC1}$,…, $\bar{v}_{DCNT}$), averaged inductor current obtained by each local controller by using DCA ($\bar{i}_{L1}$,…, $\bar{i}_{LNT}$), local measured PCC voltage with measurement error (v_{DC1}= v_{DC} ·e_{M1},…, v_{DC}·e_{MNT}) and inductor current (i_{L1},…, i_{LNT}). The outputs are duty ratios of the PWM signals for each converter (d_1,…,d_{NT}). The SS model of the controller part is formulated as:

$$\begin{cases} \dot{\mathbf{x}}_{\mathbf{ctrl}}(t) = \mathbf{A.ctrl} \cdot \mathbf{x}_{\mathbf{ctrl}}(t) + \mathbf{B.ctrl} \cdot \mathbf{u}_{\mathbf{ctrl}}(t) \\ \dot{\mathbf{y}}_{\mathbf{ctrl}}(t) = \mathbf{C.ctrl} \cdot \mathbf{x}_{\mathbf{ctrl}}(t) + \mathbf{D.ctrl} \cdot \mathbf{u}_{\mathbf{ctrl}}(t) \end{cases} \tag{18}$$

$$\begin{aligned} \mathbf{x}_{\mathbf{ctrl}}(t) &= \left[\cdots \quad x_{SVi}(t) \quad x_{SCi}(t) \quad x_{Vi}(t) \quad x_{Ci}(t) \quad \cdots\right] \\ \mathbf{u}_{\mathbf{ctrl}}(t) &= \left[V^* \quad \bar{\mathbf{v}}_{\mathbf{DC}}(t) \quad \bar{\mathbf{i}}_{\mathbf{L}}(t) \quad \mathbf{i}_{\mathbf{L}}(t) \quad \mathbf{v}_{\mathbf{DC}}(t)\right] \\ \bar{\mathbf{v}}_{\mathbf{DC}}(t) &= \left[\bar{v}_{DC1}(t) \quad \bar{v}_{DC2}(t) \quad \cdots \quad \bar{v}_{DCNT}(t)\right] \\ \bar{\mathbf{i}}_{\mathbf{L}}(t) &= \left[\bar{i}_{L1}(t) \quad \bar{i}_{L2}(t) \quad \cdots \quad \bar{i}_{LNT}(t)\right] \\ \mathbf{i}_{\mathbf{L}}(t) &= \left[i_{L1}(t) \quad i_{L2}(t) \quad \cdots \quad i_{LNT}(t)\right] \\ \mathbf{v}_{\mathbf{DC}}(t) &= \left[v_{DC1}(t) \quad v_{DC2}(t) \quad \cdots \quad v_{DCNT}(t)\right] \end{aligned} \tag{19}$$

where $\mathbf{x}_{\mathbf{ctrl}i}$ is the state vector of the i^{th} controller, as four PI controllers are included corresponding to 4 states: secondary voltage and current loop states (x_{SVi} and x_{SCi}), and inner voltage and current loop states (x_{Vi} and x_{Ci}).

Moreover, considering the facts that digital controller has fixed sampling time (T_d), the controller model needs to be discretized to equivalent DT model so as to accurately represent the control system. Since trapezoidal rule based PI controllers are used for each control loop, *Tustin approximation* [28] is applied for transform controller from a CT form to a DT form. T_d=5e^{-5}s is considered as the sampling time of the digital controller.

C. Communication part

The model of the communication algorithm is shown in Fig. 3. The inputs of the communication part model ($G_{ca}(z)$) are the initial states of each node ($x_i(0)$, i=1,2,…,N_T) which are locally measured voltage and current. The outputs are the states reached in each node at k^{th} iteration ($x_i(k)$). The state variables include the cumulative differences between node i and j ($\delta_{ij}(k+1)$, $j \in N_i$, N_i is the set of indexes of the agents that are connected with agent i) and the output state ($x_i(k+1)$).

Based on this scheme, and considering that the *Laplacian* matrix should also be included, (7)-(11) can be used to establish the SS model of communication part:

$$\begin{cases} \mathbf{x}_{\mathbf{CA}}(k+1) = \mathbf{A.ca} \cdot \mathbf{x}_{\mathbf{CA}}(k) + \mathbf{B.ca} \cdot \mathbf{u}_{\mathbf{CA}} \\ \mathbf{y}_{\mathbf{CA}}(k+1) = \mathbf{C.ca} \cdot \mathbf{x}_{\mathbf{CA}}(k) + \mathbf{D.ca} \cdot \mathbf{u}_{\mathbf{CA}} \end{cases} \tag{20}$$

$$\begin{aligned} \mathbf{x}_{\mathbf{CA}}(k) &= \left[\boldsymbol{\delta}_{\mathbf{i,i+1}}(k) \quad \cdots \quad \boldsymbol{\delta}_{\mathbf{i,i+N_T\text{-}1}}(k) \quad \mathbf{x}_{\mathbf{i}}(k)\right]^T \\ \mathbf{u}_{\mathbf{CA}} &= \left[\mathbf{x}_{\mathbf{1}}(0) \quad \cdots \quad \mathbf{x}_{\mathbf{N_T}}(0)\right]^T \\ \mathbf{y}_{\mathbf{CA}}(k) &= \left[\mathbf{x}_{\mathbf{1}}(k) \quad \cdots \quad \mathbf{x}_{\mathbf{N_T}}(k)\right]^T \end{aligned} \tag{21}$$

where the elements from laplacian matrix are included in **A.ca** representing the relationship of state variables. $\boldsymbol{\delta}_{i,j}(k)$ is the cumulative difference state between node i and node j. Both the voltage and current information consensus algorithms are based on this model.

D. Model integration

The overall system model can be obtained by integrating the three models: the plant part model in CT form (s domain), controller part model in DT form (z domain) with sampling time T_d, and communication part model in DT form with sampling time T_{ca}. The model integration requires proper handling of different sampling times and interfacing variables. The following steps are executed in order to obtain the accurate overall system model, as shown in Fig. 6: 1) The MG plant is modeled in CT form, however, the controller part measures voltage and current based on the measurement sampling time (T_d). The MG plant model is first discretized using ZOH method with the same sampling time of T_d; 2) Tustin method is used to transform the controller model from s domain to z domain with a sampling time T_d; 3) The combination of MG plant model and controller model can be realized by interfacing their input/output variables and closing loops. Duty ratios become inner states after combination; 4) In

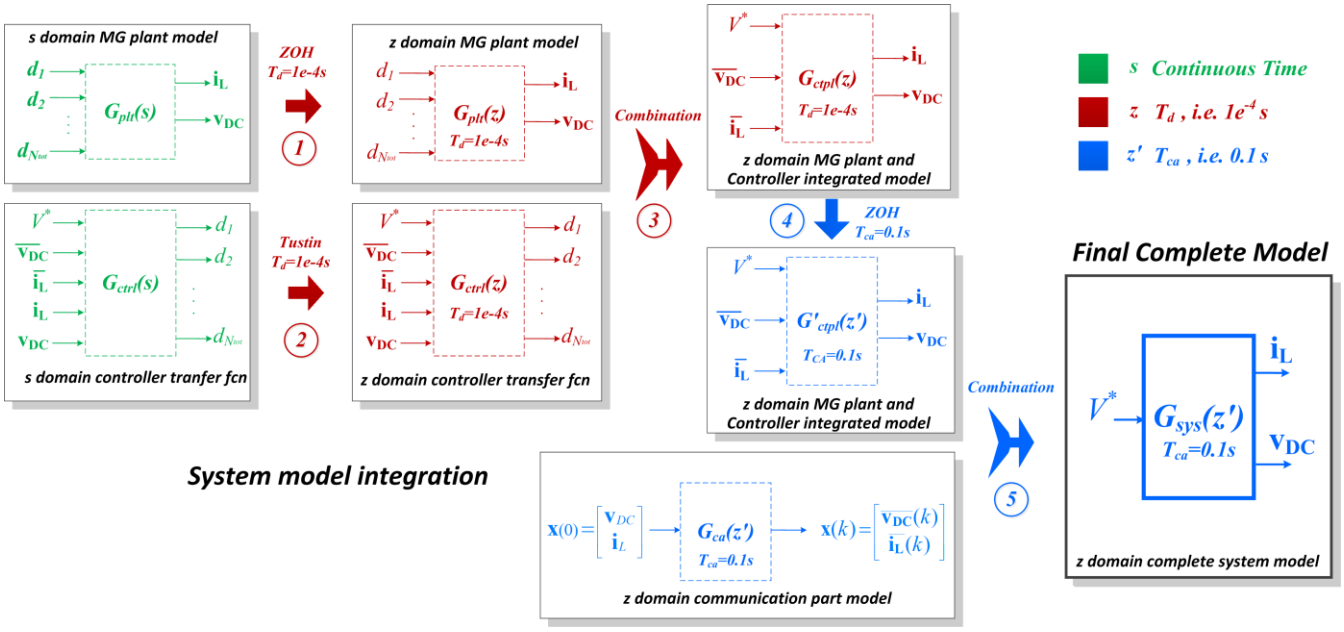

Fig. 6. System model integration.

order to integrate with communication part model, the MG plant and controller combined model is discretized using ZOH method with sampling time T_{ca}; 5) Finally, the complete system model can be obtained by integrating communication part model with MG plant and controller model under sampling time T_{ca}.

V. Sysetm Performance Evaluation

This Section presents the simulation results to test the effectiveness and performance of the applied control structure considering load change, converter fault and communication topology change. A group of paralleling buck converters is built in Plecs with the same parameters as shown in Fig. 5 (time step of 1e-6s is used to emulate the CT system). Primary and secondary control loops are implemented in Simulink with time step T_d=5e-5s. The communication links and consensus algorithm are also formulated in Simulink with time step T_{ca} which can be changed from 10ms to 1000ms. 3-unit and 6-unit systems are simulated in this Section to test the effectiveness of the proposed method. The system parameters are given in Table I.

TABLE I. Parameters of Primary and Secondary Control Loops

Priamry Control				
Virtual Resistance (Droop)	*Voltage PI Loop*		*Current PI Loop*	
R_d=0.2 Ohm	K_{pv}=4	K_{iv}=800	K_{pc}=1	K_{ic}=97
Secondary Control				
Secondary Voltage PI Loop		*Secondary Current PI Loop*		
K_{psv}=0.02	K_{isv}=2	K_{psc}=0.02	K_{isc}=1	

A. Control Activation and Load Change Dynamics

The control activation and load change dynamics in 3-unit and 6-unit system are given in Fig. 7 (a), (b) and (d). In Fig 7 (a) the communication time step is set to 100ms. Before 0.5s, the proposed control is not activated, the converters currents are not accurately shared because of feeder line differences (resistive feeder lines are considered in small scale microgrid, feeder line resistances of the three converters are set to 0.1, 0.2 and 0.3 Ohm respectively), and the voltage deviates from nominal value (48V) because of the usage of droop control and feeder line impedance. At 0.5s, the distributed secondary control is activated, the converter currents converge to average value within 1s and the PCC voltage is recovered to 48V. At 2.5s, a resistive load is connected to PCC causing the increasing of converter currents. The converter currents are kept well shared and the PCC voltage is restored within 1s. The same process is simulated in Fig. 7 (d) with 6 units.

In above cases, the units exchange information every 100ms to emulate a low bandwidth communication resulting in a convergence time around 1s. If a fast communication is considered, such as the case shown in Fig. 7 (b), units exchanges information every 20ms, the system converges within 0.3s. In real world application, the regulation speed is actually limited by the communication bandwidth as the cases shown in the simulation results.

B. Converter Fault and Unintentional Disconnection

Fig. 7 (c) simulates a converter fault condition. At 0.5s, the converter 3 is suddenly stopped and disconnected from the system, while converter 1 and 2 keep sharing the total load current. The PCC voltage appears a sudden drop right after disconnection of converter 3, but it is restored to nominal value within 1s.

C. Communication Topology Change

Fig. 7 (e) and (f) show the system response considering two different conditions of communication loss: (e) the communication topology remains connected after loss; (f) the communication topology splits to two parts after loss.

In Fig. 7 (e), the distributed secondary control is activated at 0.2s, and the system reach steady state after 1.5s. At 2s, three communication links are disconnected and the

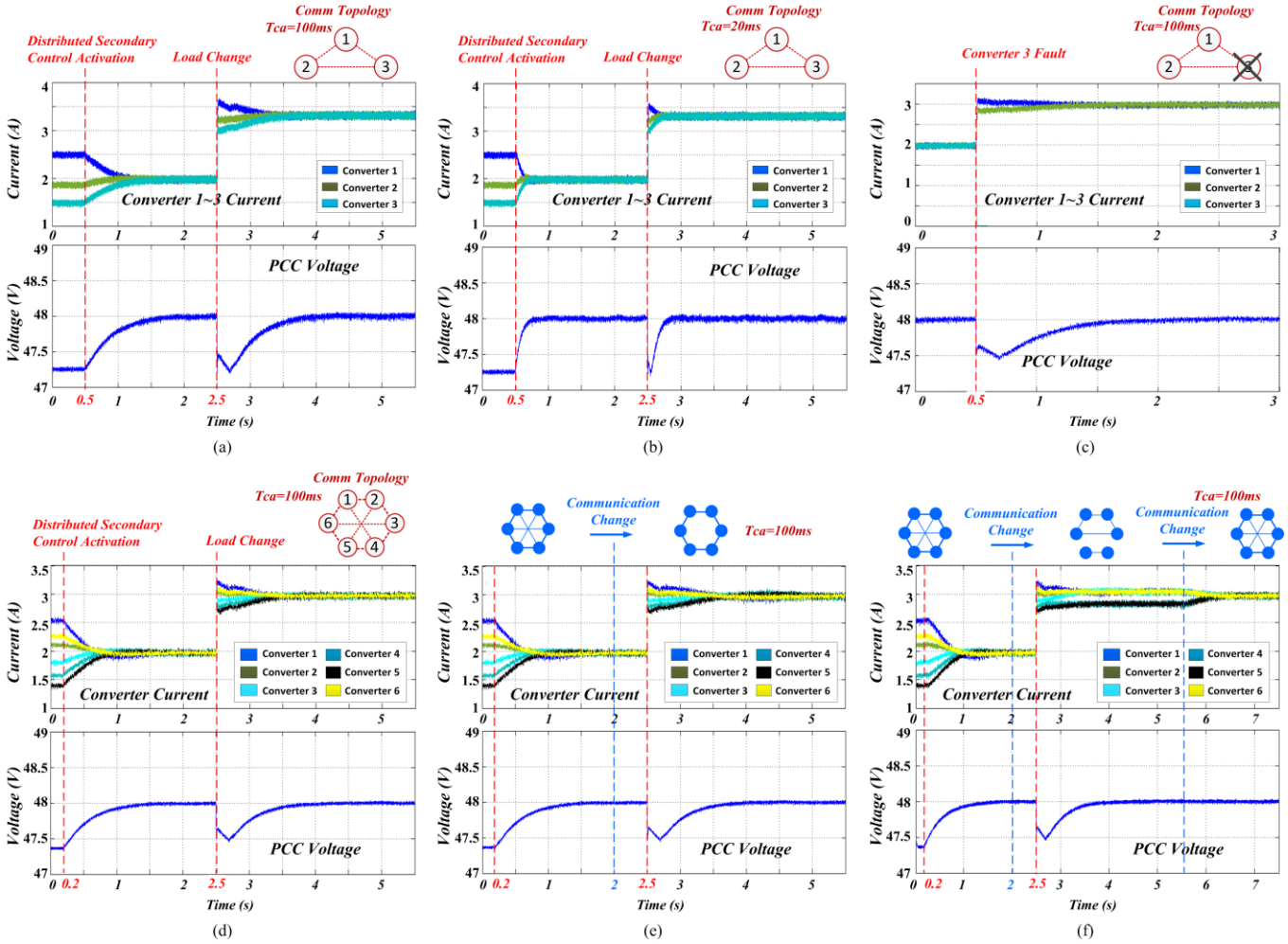

Fig. 7. System performance evaluation: (a) load change in 3-converter system; (b) Load change with different communication time step; (c) converter fault condition; (d) load change in 6-converter system; (e) communication topology change; (f) communication network split (plug-and-play function).

communication topology is change from CROSS to RING shape. Because the steady state was reached, the loss of communication link does not affect the system immediately. However, after a load change at 2.5s, the converter currents converge slower than CROSS shape case (compare the system dynamic of Fig. 7 (d) and (e) after 2.5s). The reason is that after loss of communication links, the convergence speed becomes slower (see Fig. 3 (b)) causing the slower dynamic of the system. The result indicates that the loss of communication links affects the dynamics of the system, however, if all the units still remain connected (there is still a direct/indirect path between each pair of units), the system can keep normal operation and converge to right value.

Fig. 7 (f) shows the system response to communication network split and reconnection. At 2s, the communication network splits into two parts, four units formulate a RING shape network, the other two units (converter 4 and 5) split from the main network and communicate only with each other. After loading at 2.5s, the PCC voltage is still restored to the nominal value, while converter currents of the two parts converge to different values. At 5.5s, the communication network is recovered resulting in the convergence of converter currents. The result demonstrates that after communication network split, the system can keep stable operation but the converter current sharing cannot be guaranteed. After communication system restoration, the system can recover normal operation immediately. Accordingly, plug-and-play function can be realized with the proposed method.

As a conclusion, the above results demonstrate that the proposed control algorithm has the following features: a) it realizes the accurate current sharing and voltage restoration; b) the response speed of the system depends on both the control parameters and the communication rate; c) if unit fault condition happens, the fault unit can be excluded from the system and the remaining units can keep normal operation; d) in case of communication loss, if all the units remain connected (there is at least one direct/indirect path between each pair of units), the system will continue normal operation; e) plug-and-play function is realized.

VI. Sysetm Model Verification and Sensitivity Study

This Section compares the established model with simulation results to verify the correctness of the proposed modeling approach. Base on the model, a sensitivity study is conducted. 3-unit and 6-unit systems are considered in this study in order to evaluate the system from more perspectives.

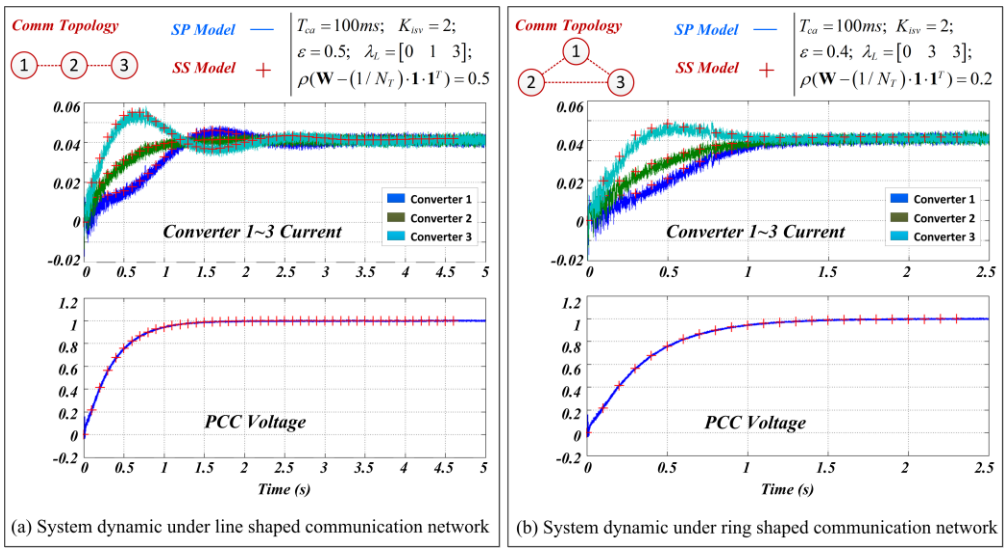

Fig. 8. 3-node system dynamic.

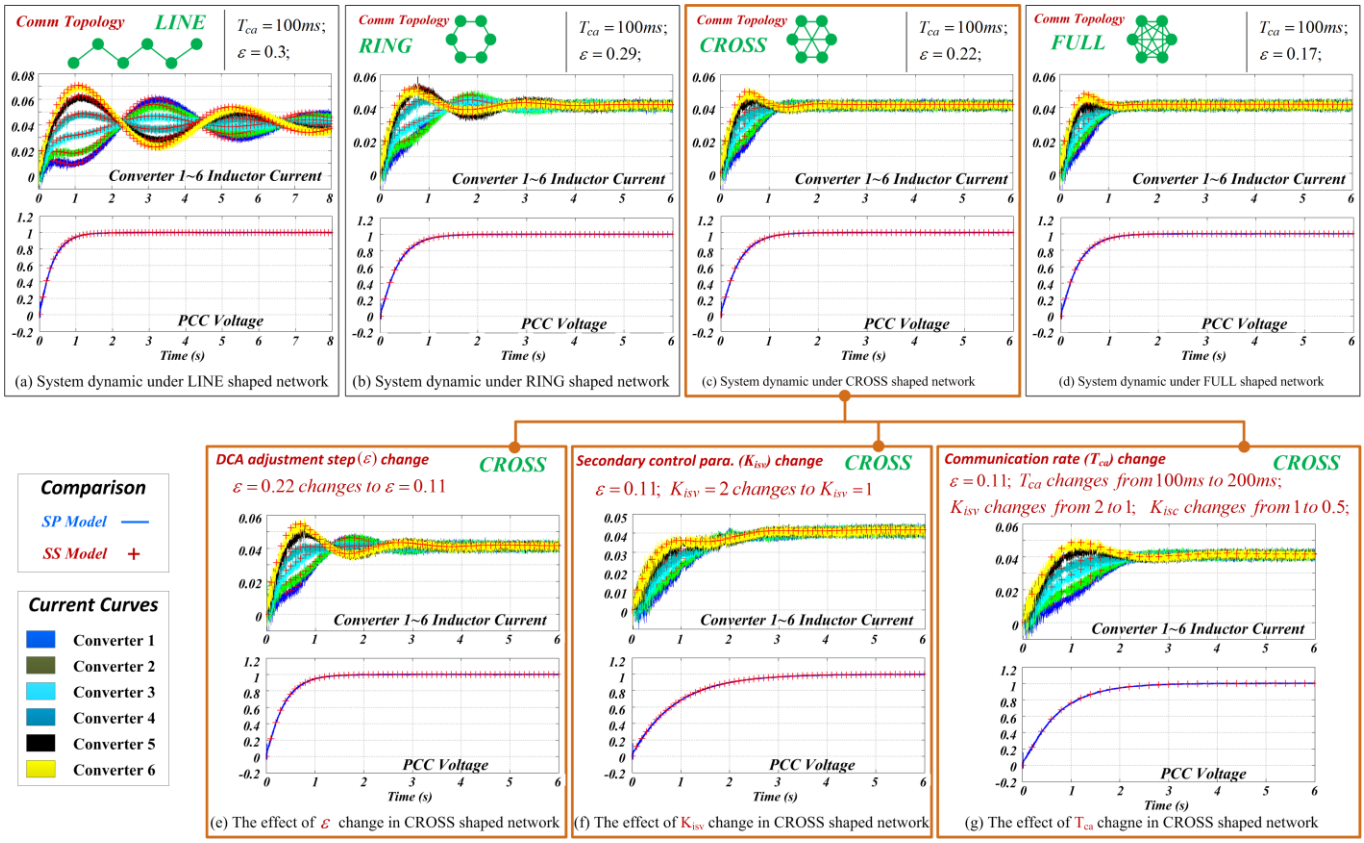

Fig. 9. 6-node system dynamic.

Emulated measurement errors (e_M) are considered in this part. In 3-unit system the measurement errors are set to: e_{M1}=+0.8%, e_{M2}=+0.2%, e_{M3}=-0.8%. In 6-unit system the measurement errors are set to: e_{M1}=+0.5%, e_{M2}=+0.3%, e_{M3}=+0.2%, e_{M4}=+0.1%, e_{M5}=-0.2%, e_{M6}=-0.5%.

First of all, the step response of the SS model is compared with the SS model to verify the correctness of the modeling approach. Then several comparison cases are studied and discussed focusing on the system dynamics under different communication topologies, consensus algorithm parameters and control parameters. Finally, conclusions are made based on the presented results.

The step response of the SS model and SP model with different system configurations are obtained as shown in Fig. 8 and Fig. 9. Both the voltage and current are divided by the rated voltage value (48V) so as to compare the dynamic of the SS model and SP model. It can be seen that with different communication topologies and control parameters the step response of the SS model fits well into the SP model, which demonstrates the correctness of the modeling method. Based

on this model, the system dynamics under different communication topologies, DCA adjustment steps, communication rate (time step), and control parameters are analyzed in the following part.

A. Topology

According to Fig. 3 (b), the topology of the communication network may significantly affect the dynamics of the information consensus. As the control loops in each local control are based on the knowledge from DCA, different communication topologies also incur distinguished system behavior, as shown in Fig. 8 and Fig. 9 (a)-(d).

In Fig. 8, a 3-node system is modeled and simulated with LINE shaped and RING shaped communication topologies. The communication rate (T_{ca}) is considered to be 100ms. Constant edge weight ε is set to 0.5 for LINE case and 0.4 for RING case which offers the minimized spectral radius $\rho(\mathbf{W}-(1/N_T)\cdot\mathbf{1}\cdot\mathbf{1}^T)$ in each case to ensure the fastest convergence of DCA. The current and voltage curves show the dynamic of the overall system which indicates that RING shaped case offers faster and more stable response compared with LINE shaped case.

In Fig. 9 (a)-(d), a 6-node system is studied. With the increasing number of communication links, the communication topology changes from LINE shape, RING shape, CROSS shape to fully connected network. In each case the fastest convergence of DCA is ensured by properly choosing ε. It can be seen from the converter current curve comparison that fast and stable system step responses are obtained under CROSS shaped and fully connected networks since they offer faster information consensus. While the RING shaped and LINE shaped cases incur more oscillation and longer response transient time. The presented results go well in line with theory previously developed in [29] that, the algebraic connectivity and convergence speed of small world networks can be significantly improved by properly design the topology of the communication network.

B. *DCA constant edge weight* ε

Apart from communication topology, the constant edge weight (ε) also has decisive influence on DCA convergence, as shown in Fig. 3 (a). In Fig. 9 (e), the CROSS case is taken as an example, the ε is changed from 0.22 to 0.11, which consequently changes $\rho\left(\mathbf{W}-(1/N_T)\cdot\mathbf{1}\cdot\mathbf{1}^T\right)$ from 0.33 to 0.67. The increased spectral radius indicates slower convergence speed of DCA that causes more oscillation and response transient time in Fig. 9 (e) compared with Fig. 9 (c). The root locus of the complete system model ($\boldsymbol{G}_{\mathbf{sys}}(z)$) is shown in Fig. 10. The constant edge weight (ε) is modified from 0.4/9 to 2.4/9. As shown in Fig. 3, the fastest convergence of DCA is obtained when 2/9, while the higher ε is, the more oscillating the DCA dyamics becomes. Also, it can be seen in Fig. 10 that, if the constant edge weight is set to a value higher than 2/9, stability can be threatened. On the other hand, although an smaller value of ε do not offer the fastest convergence, it guarantees an stable operation.

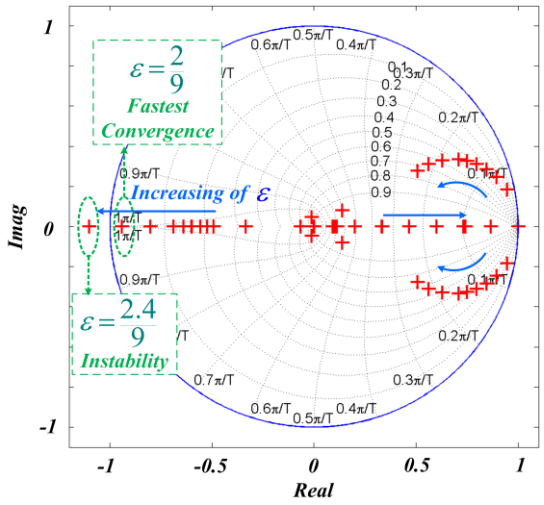

Fig. 10. Root locus with constant edge weight changing.

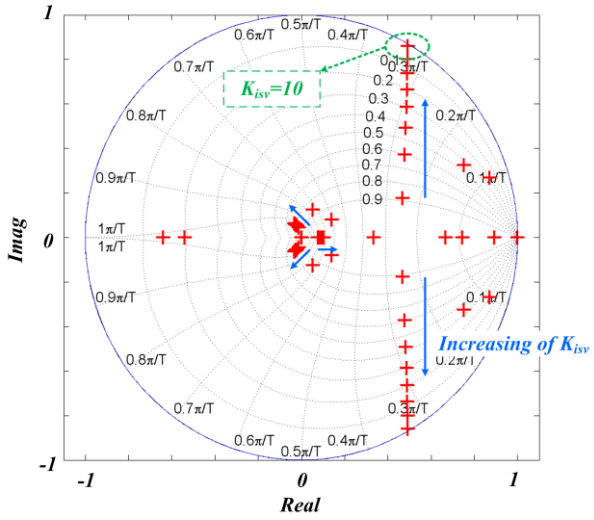

Fig. 11. Root locus with secondary parameter K_{isv} changing.

C. Secondary control parameter

Compared with inner control loops, secondary control has relative lower bandwidth and slower speed. Also considering that the performance of secondary control is based on the knowledge from DCA, this control level is more interactive between nodes and should hence be designed with respect to the communication features. As the slow convergence speed of DCA may cause oscillations (see Fig. 9 (e)) secondary controlparameters can be adjusted to help damping the system behavior. In Fig. 9 (f), the constant edge weight (ε) is set to 0.11, so the converge time is not minimum. Under this situation, the integral term of the secondary voltage controller (K_{isv}) is changed from 2 to 1 to slow down the secondary controller speed. As can be seen in Fig. 9 (f), although the response transient time becomes longer, the system dynamics becomes more damped. The root locus of the system with K_{isv} varying is shown in Fig. 11. The secondary integral term is changed from 1 to 10 under CROSS shaped network with constant edge weight $\varepsilon = 0.11$. It can be seen from the figure that with the increasing of K_{isv}, the system response becomes faster but occur to be more oscillating (decreasing of damping

factor). When K_{isv} reaches the value of 10, the system is on the edge of the stability margin. The analysis is in accordance with Fig. 9 (f) that smaller K_{isv} values help the system damping but sacrifice the response time.

D. Communication time step T_{ca}

Another practical issue in communication part is the communication rate which depends on the type of communication topology being used in the real system. In the study case, the communication rate is taken as the time step of the DCA (T_{ca}). The change of T_{ca} certainly has a significant influence on the dynamics of the overall system. In Fig. 9 (g), T_{ca} is changed from 100ms to 200ms under CROSS shaped case with $\varepsilon = 0.11$. In order to stabilize the system, the integral term of the secondary voltage and current control loops (K_{isv} and K_{isc}) are decreased from 2 to 1 and 1 to 0.5 respectively. The voltage and current values converge to the right reference values but require longer response time compared with Fig. 9 (d). The root locus and system step responses with T_{ca} changing are shown in Fig. 12. In Fig. 12, T_{ca} is changed from 100ms to 1200ms under CROSS shaped network with $\varepsilon = 0.11$ and K_{isv}/K_{isc}=1/0.5. The increasing of T_{ca} causes decreasing of system damping factor and finally incurs instability.

E. Conclusions from demonstration results

Based on the above results, the following conclusions can be obtained:

1) the correctness of the SS model is verified as the step response of the SS model accurately fits SP model;
2) the influence of communication topology on system dynamics is investigated, which indicates that the convergence speed of DCA significantly affects the dynamics of the system;
3) apart from topology, the constant edge weight (ε) also affects the convergence rate of DCA. Although smaller value of ε offers less oscillation in DCA convergence, the slow information convergence may also incur overall system oscillation (Fig. 9 (e) compared with Fig. 9 (c));
4) secondary control parameters can be adjusted to slow down or speed up the secondary control according to the communication features so as to reduce oscillation and improve system dynamics;
5) considering the communication transmission rate, it certainly has a decisive influence on the information convergence speed. Different types of communication technologies offer distinguished features, which require proper tuning of the control algorithms.

VII. Conclusion

This paper investigates the modeling method for dynamic consensus algorithm based distributed hierarchical control of DC MGs with full consideration of underlying communication topology. The hierarchical control includes inner voltage and current control loops, virtual resistance and secondary voltage

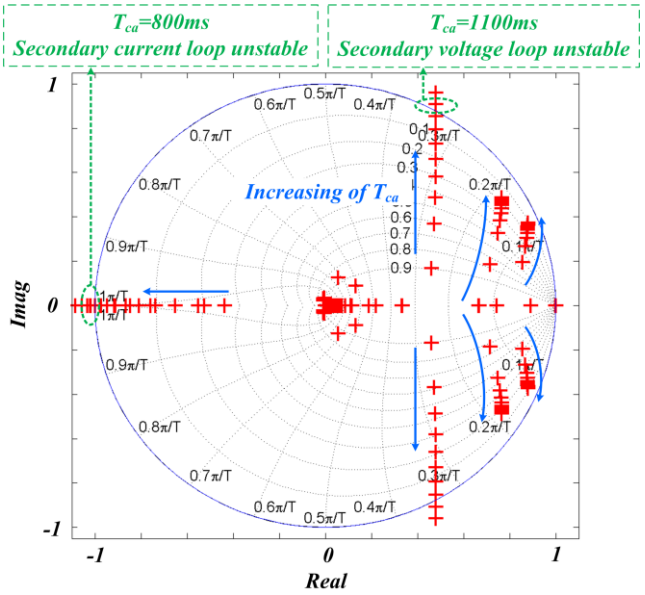

Fig. 12. System behaviour with secondary parameter *Tca* changing.

and current control loops aiming at realizing accurate current sharing and keeping rated voltage amplitude in the PCC. The performance of the secondary controller is based on the knowledge from dynamic consensus algorithm, which includes the averaged voltage and current value among all the distributed units. In this sense, the distributed units interact with each other not only through the electrical network but also the communication links. The system becomes more interactive compared with conventional centralized methods. Accordingly, this paper proposes a modeling method in discrete time domain in order to properly analyze the interactive feature of this kind of system. Taking into account the different sampling times of the plant, the digital controller and the communication devices, the system is modeled with these three parts separately. Zero order hold and Tustin methods are used to discretize the models and integrate them into a complete system state space model. By comparing with Simulink/Plecs based model, the correctness of the state space model is justified. Finally, based on this model, the system dynamics and parameter sensitivity are studied and analyzed.

VIII. References

[1] C. Committee, D. Generation, and E. Storage, *IEEE Guide for Design , Operation , and Integration of Distributed Resource Island Systems with Electric Power Systems IEEE Standards Coordinating Committee 21 Sponsored by the*. 2011, pp. 1–54.

[2] J. M. Guerrero, J. C. Vasquez, J. Matas, L. G. De Vicuna, and M. Castilla, "Hierarchical Control of Droop-Controlled AC and DC Microgrids — A General Approach Toward Standardization," *IEEE Trans. Ind. Electron.*, vol. 58, pp. 158–172, 2011.

[3] A. Bidram and A. Davoudi, "Hierarchical Structure of Microgrids Control System," *IEEE Trans. Smart Grid*, vol. 3, pp. 1963–1976, 2012.

[4] D. E. Olivares, A. Mehrizi-Sani, A. H. Etemadi, C. A. Canizares, R. Iravani, M. Kazerani, A. H. Hajimiragha, O. Gomis-Bellmunt, M. Saeedifard, R. Palma-Behnke, G. A. Jimenez-Estevez, and N. D. Hatziargyriou, "Trends in Microgrid Control," *IEEE Trans. Smart Grid*, vol. 5, no. 4, pp. 1905–1919, Jul. 2014.

[5] M. Savaghebi, A. Jalilian, J. C. Vasquez, and J. M. Guerrero, "Secondary Control for Voltage Quality Enhancement in Microgrids," *IEEE Trans. Smart Grid*, vol. 3, no. 4, pp. 1893–1902, Dec. 2012.

[6] T. Dragicevic, J. M. Guerrero, J. C. Vasquez, and D. Skrlec, "Supervisory Control of an Adaptive-Droop Regulated DC Microgrid With Battery Management Capability," *IEEE Trans. Power Electron.*, vol. 29, no. 2, pp. 695–706, Feb. 2014.
[7] Q. Shafiee, C. Stefanovic, T. Dragicevic, P. Popovski, J. C. Vasquez, and J. M. Guerrero, "Robust Networked Control Scheme for Distributed Secondary Control of Islanded Microgrids," *IEEE Trans. Ind. Electron.*, vol. 61, no. 10, pp. 5363–5374, Oct. 2014.
[8] T. Dragičević, J. M. Guerrero, and J. C. Vasquez, "A distributed control strategy for coordination of an autonomous LVDC microgrid based on power-line signaling," *IEEE Trans. Ind. Electron.*, vol. 61, pp. 3313–3326, 2014.
[9] V. Nasirian, S. Moayedi, A. Davoudi, and F. Lewis, "Distributed Cooperative Control of DC Microgrids," *IEEE Trans. Power Electron.*, vol. PP, no. 99, pp. 1–1, 2014.
[10] L. Meng, T. Dragicevic, J. M. Guerrero, and J. C. Vasquez, "Optimization with system damping restoration for droop controlled DC-DC converters," in *2013 IEEE Energy Conversion Congress and Exposition*, 2013, pp. 65–72.
[11] D. E. Olivares, C. A. Canizares, and M. Kazerani, "A centralized optimal energy management system for microgrids," in *2011 IEEE Power and Energy Society General Meeting*, 2011, pp. 1–6.
[12] A. G. Tsikalakis and N. D. Hatziargyriou, "Centralized control for optimizing microgrids operation," *IEEE Trans. Energy Convers.*, vol. 23, pp. 241–248, 2008.
[13] K. T. Tan, X. Y. Peng, P. L. So, Y. C. Chu, and M. Z. Q. Chen, "Centralized Control for Parallel Operation of Distributed Generation Inverters in Microgrids," *IEEE Transactions on Smart Grid*. pp. 1–11, 2012.
[14] A. G. Tsikalakis and N. D. Hatziargyriou, "Centralized control for optimizing microgrids operation," *2011 IEEE Power Energy Soc. Gen. Meet.*, pp. 1–8, 2011.
[15] Y. Xu and W. Liu, "Novel Multiagent Based Load Restoration Algorithm for Microgrids," *IEEE Trans. Smart Grid*, vol. 2, pp. 140–149, 2011.
[16] H. Liang, B. Choi, W. Zhuang, X. Shen, A. A. Awad, and A. Abdr, "Multiagent coordination in microgrids via wireless networks," *IEEE Wireless Communications*, vol. 19. pp. 14–22, 2012.
[17] L. Meng, T. Dragicevic, J. M. Guerrero, and J. C. Vasquez, "Dynamic consensus algorithm based distributed global efficiency optimization of a droop controlled DC microgrid." pp. 1276–1283, 2014.
[18] R. Olfati-Saber, J. A. Fax, and R. M. Murray, "Consensus and Cooperation in Networked Multi-Agent Systems," *Proc. IEEE*, vol. 95, 2007.
[19] S. Sučić, J. G. Havelka, and T. Dragičević, "A device-level service-oriented middleware platform for self-manageable DC microgrid applications utilizing semantic-enabled distributed energy resources," *Int. J. Electr. Power Energy Syst.*, vol. 54, pp. 576–588, 2014.
[20] M. Kriegleder, "A Correction to Algorithm A2 in 'Asynchronous Distributed Averaging on Communication Networks,'" vol. PP, no. 99. p. 1, 2013.
[21] Y. Huang and C. K. Tse, "Circuit theoretic classification of parallel connected dc-dc converters," *IEEE Trans. Circuits Syst. I Regul. Pap.*, vol. 54, pp. 1099–1108, 2007.
[22] S. L. S. Luo, Z. Y. Z. Ye, R.-L. L. R.-L. Lin, and F. C. Lee, "A classification and evaluation of paralleling methods for power supply modules," *30th Annu. IEEE Power Electron. Spec. Conf. Rec. (Cat. No.99CH36321)*, vol. 2, 1999.
[23] R. Olfati-Saber and R. M. Murray, "Consensus Problems in Networks of Agents With Switching Topology and Time-Delays," *IEEE Trans. Automat. Contr.*, vol. 49, no. 9, pp. 1520–1533, Sep. 2004.
[24] R. Merris, "Laplacian matrices of graphs: a survey," *Linear Algebra and its Applications*, vol. 197–198. pp. 143–176, 1994.
[25] N. Biggs, *Algebraic Graph Theory, Cambridge Tracks in Mathematics*. Cambridge, U.K.: Cambridge Univ. Press, 1974.
[26] C. Godsil and G. Royle, *Algebraic Graph Theory*, Vol. 207. New York: Springer-Verlag, 2001.
[27] L. X. L. Xiao and S. Boyd, "Fast linear iterations for distributed averaging," *42nd IEEE Int. Conf. Decis. Control (IEEE Cat. No.03CH37475)*, vol. 5, 2003.
[28] B. C. Kuo, *Digital control systems*, 2nd. oath. Forth Worth: Harcourt Brace, 1992.
[29] R. Olfati-Saber, "Ultrafast consensus in small-world networks," in *Proceedings of the 2005, American Control Conference, 2005.*, 2005, pp. 2371–2378.

IX. Biographies

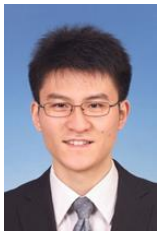

Lexuan Meng (S'13) received the B.S. degree in Electrical Engineering and M.S. degree in Electrical Machine and Apparatus from Nanjing University of Aeronautics and Astronautics (NUAA), Nanjing, China, in 2009 and 2012, respectively. He is currently working toward his Ph.D. in power electronic systems at the Department of Energy Technology, Aalborg University, Denmark, as part of the Denmark Microgrids Research Programme (www.microgrids.et.aau.dk).
His research interests include the energy management system, secondary and tertiary control for microgrids concerning power quality regulation and optimization issues, as well as the applications of distributed control and communication algorithms.

Tomislav Dragicevic (S'09-M'13) received the M.E.E. and the Ph.D. degree from the Faculty of Electrical Engineering, Zagreb, Croatia, in 2009 and 2013, respectively. Since 2010, he has been actively cooperating in an industrial project related with design of electrical power supply for remote telecommunication stations. Since 2013 he has been a fulltime Post-Doc at Aalborg University in Denmark. His fields of interest include modeling, control and energy management of intelligent electric vehicle charging stations and other types of microgrids based on renewable energy sources and energy storage technologies.

Javier Roldán-Pérez received a B.S. degree in industrial engineering, a B.S. degree in electronics and control systems, a M.S. degree in system modelling, and a Ph.D. degree in system modelling, all from Comillas Pontifical University, Madrid, in 2009, 2010, 2011, and 2015, respectively.
From 2010 to 2015 he worked in the Institute for Research in Technology (IIT), at Comillas University, developing his Ph.D. and working in research projects related to power electronics. In 2014, he was a visiting Ph.D. student at the Department of Energy Technology, Aalborg University, Denmark. Since 2015 he is working at Norvento Energía Distribuída, in the electrical and control systems department. His research interests are control systems and power electronics, including microgrid modelling and control, design and control of VSC-based technologies like Dynamic Voltage Restorers, Static Compensators, or Active Power Filters, and renewable energy sources like wind and solar.

Juan C. Vasquez (M'12-SM'15) received the B.S. degree in Electronics Engineering from Autonomous University of Manizales, Colombia in 2004 where he has been teaching courses on digital circuits, servo systems and flexible manufacturing systems. In 2009, He received his Ph.D degree on Automatic Control, Robotics and Computer Vision from the Technical University of Catalonia, BarcelonaTECH, Spain at the Department of Automatic Control Systems and Computer Engineering, where he worked as Post-doc Assistant and also teaching courses based on renewable energy systems, and power management on ac/dc minigrids and Microgrids. Since 2011, he has been an Assistant Professor in Microgrids at the Department of Energy Technology, Aalborg University, Denmark, and he is co-responsible of the Microgrids research programme co-advising more than 10 PhD students and a number of international visitors in research experience. Dr Juan Vasquez is member of the Technical Committee on Renewable Energy Systems TC-RES of the IEEE Industrial Electronics Society and the IEC System Evaluation

Group SEG 4 work on LVDC Distribution and Safety for use in Developed and Developing Economies. He is a visiting scholar at the Center for Power Electronics Systems – CPES at Virginia Tech, Blacksburg, VA, USA. He has published more than 100 journal and conference papers and holds a pending patent. His current research interests include operation, energy management, hierarchical and cooperative control, energy management systems and optimization applied to Distributed Generation in AC/DC Microgrids.

Josep M. Guerrero (S'01-M'04-SM'08-FM'15) received the B.S. degree in telecommunications engineering, the M.S. degree in electronics engineering, and the Ph.D. degree in power electronics from the Technical University of Catalonia, Barcelona, in 1997, 2000 and 2003, respectively. Since 2011, he has been a Full Professor with the Department of Energy Technology, Aalborg University, Denmark, where he is responsible for the Microgrid Research Program. From 2012 he is a guest Professor at the Chinese Academy of Science and the Nanjing University of Aeronautics and Astronautics; from 2014 he is chair Professor in Shandong University; and from 2015 he is a distinguished guest Professor in Hunan University.

His research interests is oriented to different microgrid aspects, including power electronics, distributed energy-storage systems, hierarchical and cooperative control, energy management systems, and optimization of microgrids and islanded minigrids. Prof. Guerrero is an Associate Editor for the IEEE TRANSACTIONS ON POWER ELECTRONICS, the IEEE TRANSACTIONS ON INDUSTRIAL ELECTRONICS, and the IEEE Industrial Electronics Magazine, and an Editor for the IEEE TRANSACTIONS on SMART GRID and IEEE TRANSACTIONS on ENERGY CONVERSION. He has been Guest Editor of the IEEE TRANSACTIONS ON POWER ELECTRONICS Special Issues: Power Electronics for Wind Energy Conversion and Power Electronics for Microgrids; the IEEE TRANSACTIONS ON INDUSTRIAL ELECTRONICS Special Sections: Uninterruptible Power Supplies systems, Renewable Energy Systems, Distributed Generation and Microgrids, and Industrial Applications and Implementation Issues of the Kalman Filter; and the IEEE TRANSACTIONS on SMART GRID Special Issue on Smart DC Distribution Systems. He was the chair of the Renewable Energy Systems Technical Committee of the IEEE Industrial Electronics Society. In 2014 he was awarded by Thomson Reuters as Highly Cited Researcher, and in 2015 he was elevated as IEEE Fellow for his contributions on "distributed power systems and microgrids."